RSC Advances

ROYAL SOCIETY OF CHEMISTRY

www.rsc.org/advances

Graphene oxide/polyaniline/polypyrrole nanocomposite for a supercapacitor electrode

Kaushik Pal[1], Vinay Panwar[1], Souvik Bag[1], James Manuel[2], Jou-Hyeon Ahn[2], Jin Kuk Kim[3]

[1]Department of Mechanical and Industrial Engineering, Indian Institute of Technology Roorkee-247667, India

[2]Department of Chemical and Biological Engineering, and Research Institute for Green Energy Convergence Technology, Gyeongsang National University, 900, Jinju-660701, Republic of Korea

[3]Department of Polymer Science & Engineering, Gyeongsang National University, 900, Jinju-660701, Republic of Korea

Abstract

Graphene oxide based nanocomposites were prepared through in-situ polymerization of aniline and pyrole to study the interaction of graphene oxide with polyaniline (PANI) and polypyrole (PPy). Field emission scanning electron microscopy (FESEM) was used to study the surface morphology and transmission electron microscopy (TEM) for the qualitative understanding of the internal structure of PANI/PPy coating on GO. The chemical structures of composites were studied through X-ray photoelectron spectroscopy (XPS) analysis. It was observed that, specific capacitance of PPy coated GO improved by ~122.73% comparing to pristine GO. Also, the binding energy of polypyrole-graphene oxide was found to be higher than polyaniline-graphene oxide due to the absence of oxygen containing functional groups. In addition, the storage capacity was effectively improved due to the synergistic effect of polypyrole coating on graphene oxide.

Key words: Supercapacitor electrode; Polypyrrole; Polyaniline; Graphene oxide; Cyclic voltammetry; Raman spectroscopy.

Introduction:

The electron transfer between the plates of a conventional capacitor introduces a potential difference which is mainly responsible for the storage of electrical energy. Dielectric breakdown limits the transfer of electrons and thus storage of energy. This corresponds for the dependency of stored energy on the properties of plate material. Supercapacitors provides a bridge between the batteries and thus much popular than conventional

capacitors over past few decades. These supercapacitors lead to longer life cycle, unusual high energy density and highly reduced charge separation [1]. In supercapacitors, two common energy storage mechanisms are Pseudocapacitance and Electrical double-layer (EDL) capacitance. In EDL capacitors, high surface area composed carbon based materials are generally used which assists for the accumulation of charge at the interface of electrode and electrolyte. However, in case of pseudocapacitors the electrodes are prepared using conducting polymers and metal oxides due to their rapid and reversible faradic redox reaction [2].

To achieve high capacitances, different polymers like polyaniline (PANI) [2], polypyrole (PPy) [1], and polythiophenes (PThs) [3] are widely used as supercapacitor electrodes. However, they were found quite unstable throughout the charge-discharge process. Now researchers are going on to improve the efficiencies of super capacitors using polymers and various types of nano materials like carbon nanotubes (CNT), graphene and other carbon nanomaterials.

The introduction of multi-walled carbon nanotubes (MWCNT) in 1991 by scientist S. Ijima [4], MWCNT has shown marked importance in the field of sensing, strengthening of material, energy etc. Carbon nanotubes were proved to be highly electroactive for carbon based supercapacitor electrode due to their excellent electrical conductivity [5-7]. Besides the high stability of CNTs and other carbon materials, their capacitance is limited due to their microstructures [8-11]. Meng et al. revealed that CNT/PANI composites shown superior electrochemical performance under different current loads [12]. Similar improvement in electrochemical properties have been noticed through supercapacitor electrodes prepared from combination of CNTs and conducting polymer which offer high capacitances and improved stability due to outstanding conducting properties of CNTs and high pseudocapacitance of the conducting polymer [13-16]. However, the applications of CNTs are limited in this field due to its high cost and electric double-layer capacitance limited to 80 F/g [17].

Graphene is another important advanced carbon material for supercapcitor applications due to its excellent electrical conductivity resulting from π-π interaction of sp^2 hybridized carbon atoms, ease of synthesis, remarkable mechanical stiffness and large surface area. For supercapacitor applications, graphene based nanomaterials were combined with conducting polymers like PANI and PPY. The electrochemical capacitance of graphene/PANI composite paper was observed to be 233 F/g [18]. However, Biswas et al. had observed the specific capacitance to be 164 F/g using PPy-graphene multilayered composite. This had been noticed that due to agglomeration tendency of graphene the dominating factor for capacitance for PANI-graphene surface was pseudocapacitance and not the EDL capacitance of graphene sheet. In case of graphene oxide (GO) doped PANI composites, the conductivity was highest for 1% GO doping and reduces afterwards [19].

In this work, our primary aim is to prepare GO/PANI or GO/PPy composites and study their physical and chemical properties to ensure if these can be applied as cathode material for lithium ion batteries or super capacitors.

2. Experimental

Preparation of GO

GO has been purchased from N-barotech Company, South Korea having the 95% purity. The size of GO particles was 300-800nm and the thickness was around 0.7-1.2 nm.

Preparation of PANI

10 ml of purified aniline (Aldrich) by distillation under reduced pressure was dissolved in 200 ml of 1 M HCl and cooled to 0 °C using ice bath. A solution of 6.2 g of ammonium persulphate (APS) in 100 mL 1 M HCl was slowly added to the starting solution through mechanical stirring. The polymerization reaction further proceeded by stirring for 24 h at room temperature. The resultant green colored PANI was first filtered and then washed successively with water, ethanol and acetone to eliminate the unreacted starting materials and oligomers. PANI was dried in two steps, initially at 60 °C for 12 h and then under vacuum for 24 h at 80 °C.

Preparation of PANI-GO composites

PANI-GO composites were prepared through in-situ polymerization process where PANI was uniformly coated over GO particles suspended in acidic solution. The schematic for the preparation of PANI-GO composite is presented in Figure 1. Aniline and GO were taken in 4:1 ratio and the resulting composite was named as PAG. Initially, a 0.3 M solution was prepared by dissolving purified aniline in 1 M HCl and then GO was dispersed in this solution by step sonication for around 40 minutes. Now, a solution of APS and aniline with molar ratio 1:4 was prepared in 1 M HCl and this solution was rapidly poured into the initial mixture. After around 10 minutes the color of solution turns towards green which indicate the initiation of polymerization. The solution was then allowed to stir at room temperature for 24 h and then diluted by water. Finally the composite was collected by filtration and then washed successively with 1:10 HCl solution (three times), water, ethanol and acetone until the filtrate turn out to be colorless. The actual mass percentage of the PANI in the composite is estimated by difference in weight of GO before and after polymerization and found to be around 58% by weight.

Figure 1. Schematic representation for the fabrication process of PANI-GO/PPy-GO composites.

Preparation of PPy

PPy was prepared through rapid mixing reaction [2]. In this process, the oxidation impurities were first removed by distillation of pyrrole under vacuum. Then, an aqueous solution of $FeCl_3$ (100 ml, 0.01 mol) was added to 5 g of purified pyrrole monomer dispersed in 100 mL ethanol at ~ 5 °C with vigorous magnetic stirring. The solution was kept stirring for 24 h for complete polymerization. As prepared PPy was finally filtered out and washed with deioniozed water. Precipitate was dried in two steps first at 60 °C for 12 h and then at 70 °C under vacuum.

Preparation of PPy-GO composites

PPy-GO composites were prepared in the same fashion as PANI-GO composites, through in-situ polymerization process where PPy was uniformly coated over GO particles suspended in acidic solution. Pyrrole and GO were also taken in 4:1 ratio and the resulting composite was named as PAG. Here, GO was made to wet with pyrrole monomer and then added to a solution of $FeCl_3.6H_2O$ (1.353 g) in 100 ml of ethanol under magnetic stirring at room temperature. The polymerization reaction continued for 24 h with constant magnetic stirring. The resultant GO/PPy composite was collected by filtration and then washed successively with 1:10 HCl solution (three times), water, ethanol and acetone. Precipitate was dried in two steps first at 60 °C for 6 h and then at 70 °C under vacuum for 24 h.

Cell assembly

Two-electrode electrochemical Swagelok cells were assembled with lithium metal (300 µm thickness, Cyprus Foote Mineral Co.) as anode, Celgard® 2200 separator, 1 M $LiPF_6$, in ethylene carbonate (EC) and dimethyl carbonate cathode (DMC) (1:1 v/v) electrolyte and G, PAG, or PPG composites as cathode. The cell assembly was performed under argon atmosphere in a glove box with H_2O level <10 ppm.

Characterization techniques

Electrode preparation

The electrode was prepared by mixing graphene, graphene/PANI or graphene/PPy with binder poly(vinylidene fluoride) (PVdF) in 90:10 weight ratio. The ingredients were mixed together in a stainless steel container of high energy ball milling machine with 3 zirconia balls (5 mm diameter) for 45 min at room temperature to get homogeneous slurry. The slurry was cast on aluminum foil and dried at 60 °C for 12 h and then dried further at 80 °C under vacuum for 24 h to get the film of about 34 µm thickness. The film was cut into circular discs of 1 cm diameter for use as electrode in Li battery.

Cyclic voltammetry

Cyclic voltammetry (CV) tests were carried out on an automated galvanostatic charge-discharge unit (WBCS3000 battery cycler), from 0 to 3 V at scan rate of 0.5 mV s^{-1}. We have prepared the GO composites to ensure there suitability as cathode and thus tested CV with normal scanning rate in order to study the oxidation reduction potentials. All these tests were carried out on room temperature.

XPS

The chemical structure of G, PAG, and PPG were evaluated through X-ray photoelectronic spectroscopy (XPS). This analysis was done on XPS-PHI 5500 spectrometer to investigate the chemical structures of G, PAG, and PPG. Al K_{α} (1485.6 eV) at anode voltage 13.8 kV, was used as X-ray source.

Raman spectroscopy

Raman spectrums were recorded from 50 cm^{-1} to 2950 cm^{-1} on RM2000 microscopic confocal Raman spectrometer (Renishaw in Via Plus, England). It uses a CCD detector and laser beam of He-Ne having 514 nm wavelength. It provides structural information about carbon-based materials.

Surface morphology and internal structure

The surface morphology of composites was explored through field emission scanning electron microscopy (FESEM) "FESEM JEOL JSM" (pressure: 10^{-6} mBar). Secondary Electron (SE) detector was used for analyzing the electrons and gold is used for the coating of polymer specimen. Transmission electron microscopy (TEM) analysis was conducted on "JEOL JEM-2010" microscope at a voltage of 200 kV to study the internal structure of composites.

Results and discussions

Cyclic voltammetry

Figure 2(a), (b) and (c) shows CV curves of GO, PAG, and PPG at a constant scan rate of 0.5 mV s^{-1} and voltage 0-3 V. From the CV curve, broad oxidation and reduction peaks have been identified which signify an efficient reversible intercalation of lithium ion into GO towards 0 V. Moreover, the CV curves for GO shown in Figure 2(a) seems to be almost flat having small redox peaks, which may be due to the high internal as well as interfacial resistance of electrode material. However, a fast current response is observed in applied voltage range which signifies the presence of electrical double-layer

capacitance [1]. In figures 2b and 2c, it has been observed that with coating PANI or PPY on GO particals the redox peaks are much higher than pristine GO. This reveals the presence of pseudocapacitance in PANI-GO and PPy-GO composites. The specific capacitance of composites is calculated using following equation

$$C = \frac{I \times \Delta t}{\Delta V \times m}$$

where, I is current (A), Δt is discharge time (sec), ΔV is potential change during discharge (V) and m is the mass of active material of electrode (gm). This has been observed that the specific capacitance improves by ~95.45% (220-430 F/g) with addition of PANI. However, PPy coating over GO increases its specific capacitance by ~122.73% (220-490 F/g). It may be due to the two redox peaks in PPy-GO which resulted in its higher specific capacitance than PANI-GO [20-21]. This clearly reveal the effectiveness of PPy coating over GO for their applications in supercapacitors.

Also, the homogeneous dispersion in case of PPy-GO, as can be observed through FESEM image, decreases the diffusion and migration length of the electrolyte ions which results in rapid charge-discharge process and improved discharge capacity than PANI-GO due to higher negative current density. The conductivity of GO encourages its applications in composites, as it serves to provide highly conductive path and a supporting material with large surface area [22]

Figure 2. Cyclic voltammetry (CV) curves of (a) GO, (b) PAG, and (c) PPG.

Raman Spectroscopy:

Raman spectroscopy of GO, PAG, and PPG are shown in Figure 3. The most distinguishing factor for raman spectra of pure GO and their nanocomposites is the peaks for D and G bands. In Figure 3, the D and G bands of GO are observed at 1355 cm^{-1} and 1597 cm^{-1} raman shift, respectively. This corresponds to the well-documented D and G bands for GO. The difference in the intensity of two bands indicates the presence of defect in pure graphene [23]. Apart from existing D and G bands of GO, two new peaks at 1164 cm^{-1} and 1492 cm^{-1} are observed due to presence of PANI structures corresponding to the $C\text{-}N^{+}$ and C=N stretching respectively [24]. However, according to the Raman spectrum of the PPG nanocomposite, the D and G bands have significantly broadened and also been shifted to 1330 cm^{-1} and 1590 cm^{-1} respectively which corroborates the enhanced interaction among GO and PPy as compared to the combination of GO and PANI.

Moreover, the I_D/I_G ratios for GO, PAG and PPG are noted to be 0.92, 0.80 and 0.85, respectively. The increment in intensity ratio of PPG composites may be attributed to the increased number of sp^2 domains formed during the in-situ polymerization process or reduction in disordered crystal structure of composites.

Figure 3. Raman spectroscopy of GO, PAG, and PPG composites.

XPS analysis

XPS was used for analyzing the chemical structure of GO, PAG and PPG composites. Figure 4 represents corresponding results through exploring the peaks at particular range of binding energy which confirms the presence of various elements and their relative intensities. The XPS spectrum of GO within the binding energy range of 0 to 1200 eV is presented in Figure 4(a). The broad scan of the GO spectrum corroborates the presence of carbon and oxygen with C/O ratio of 1.87. The similar chemical composition of GO is also reported elsewhere where the C/O ratio is around 2 [25-26]. The GO spectrum in N1s region (400 eV) of GO composite reveals that the nitrogen content in GO is less than 0.1 wt%.

After PANI was added to GO, the broad scan spectrum of PAG shows a new peak around 400 eV in Figure 4(b). This new peak is attributed to N1s component for which the C/O ratio of PAG was again found to be 1.87. This shows that there is no further addition of carbon atoms due to addition of PANI. The XPS spectrum of PPG, shown in Figure 4(c), clearly indicates an increase in area under curve due to enhanced N1 peak. This increase in area signifies the improvement in binding energy among the components. Generally these N1 peaks are combination of three Gaussian peaks comprising of 398.2, 399.9 and 401.2 eV binding energy [27]. A close observation of these peaks according to the area of the peak reveals the successful elimination of oxygen containing functional at higher extent in case of PPG composites [28].

Figure 4. X-ray photoelectron spectroscopy (XPS) of composites (a) GO, (b) PAG, and (c) PPG.

Structure and surface morphology

FESEM and TEM were used for the study of surface morphology and qualitative understanding of the internal structure of GO, PANI, PAG, and PPG. Corresponding

results are shown in Figures 5 and 6, respectively. FESEM results depicted from Figure 5 illustrates that, polymerization of PANI with GO represented as PAG form worm like aggregates having ~290 nm diameter and 6-8 μm length. It is clear from SEM image that dispersion of PANI coated GO particles is non-uniform and the coated particles are found as agglomerations in composite at different sites. However, in case of PPG composites the dispersion is much more uniform and agglomeration free as can be visualized through the inserts in SEM image of PPG.

The TEM images shown in Figure 6 reveal the improvement in network formation with coating of PANI or PPY on GO particles. A core shell modification is observed in both PAG and PPG composites. The uniformity of coating on GO is noticed to be more in case of PPy coated GO particles shown in Figure 6(c). Similar observation has been made earlier where the core structures remained unchanged but their surfaces were modified [29].

Figure 5. Representative SEM images of **(a)** GO, **(b)** PAG, and **(c)** PPG.

Figure 6. Representative TEM images of **(a)** GO, **(b)** PAG, and **(c)** PPG.

Conclusions

In this paper, graphene, GO/PANI and GO/PPy composites were synthesized using in-situ polymerization. The shifting of characteristic peaks in Raman spectra of GO/PPy composites to lower wave numbers as compared to pure GO or PAG composites revealed the effectiveness of doping. From cyclic voltammetry, it has been clearly observed that for supercapacitor electrodes the coating of PPy is much better than PANI coating on GO particles due to improved discharge capacity and higher specific capacitance. Furthermore, it has been clearly observed through morphological analysis that PPG composites show improved uniformity in coating with reduced agglomeration and better networking in comparison to PAG composites.

References

1. S. Bose, N. H. Kim, T. Kuila, K. Lau and J. H. Lee, *Nanotechnology*, 2011, **22**, 295202.
2. K. Zhang, L. L. Zhang, X. S. Zhao and J. Wu, *Chem. Mater.*, 2010, **22**, 1392.
3. T. M. Wu, H. L. Chang and Y. W. Lin, *Compos. Sci. Technol.*, 2009, **69**, 639.
4. S. Iijima, *Nature*, 1991, **354**, 56.
5. C. G. Liu, M. Liu, F. Li and H. M. Cheng, *Appl. Phys. Lett.*, 2008, **92**, 143108.
6. M. M. Shaijumon, F. S. Ou, L. Ci and P. M. Ajayan, *Chem. Commun.*, 2008, **20**, 2373.
7. B. J. Yoon, S. H. Jeong, K. H. Lee, H. S. Kim, C. G. Park and J. H. Han, *Chem. Phys. Lett.*, 2004, **388**, 170.
8. D. N. Futaba, K. Hata, T. Yamada, T. Hiraoka, Y. Hayamizu, Y. Kakudate, O. Tanaike, H. Hatori, M. Yumura and S. Iijima, *Nat. Mater.*, 2006, **5**, 987.
9. C. Portet, J. Chmiola, Y. Gogotsi, S. Park and K. Lian, *Electrochim. Acta*, 2008, **53**, 7675.
10. C. M. Yang, Y. J. Kim, M. Endo, H. Kanoh, M. Yudasaka, S. Iijima and K. Kaneko, *J. Am. Chem. Soc.*, 2007, **129**, 20.
11. L. L. Zhang, and X. S. Zhao, "Carbon-based materials as supercapacitor electrodes," *Chem. Soc. Rev.*, vol. 38, pp. 2520-2531, Jun. 2009.
12. C. Meng, C. Liu , and S. Fan, *Electrochem. Commun.*, 2009, **11**, 186.
13. L. B. Kong, J. Zhang, J. J. An, Y. C. Luo and L. Kang, *J. Mater. Sci.*, 2008, **43**, 3664.
14. S. R. Sivakkumar, W. J. Kim, J. A. Choi, D. R. MacFarlane, M. Forsyth and D. W. Kim, *J. Power Sources*, 2007, **171**, 1062.
15. H. Y. Mi, X. G. Zhang, S. Y. An, X. G. Ye and S. D. Yang, *Electrochem. Commun.*, 2007, **9**, 2859.
16. E. Frackowiak, V. Khomenko, K. Jurewicz, K. Lota and F. Beguin, *J. Power Sources*, 2006, **153**, 413.
17. C. Niu, E. K. Sichel, R. Hoch, D. Moy and H. Tennent, *Appl. Phys. Lett.*, 1997, **70**, 1480.
18. D. W. Wang, F. Li, J. Zhao, W. Ren, Z.-G. Chen, J. Tan, Z.-S. Wu, I. Gentle, G. Q. Li and H.-M. Cheng, *ACS Nano*, 2009, **3**, 1745.
19. H. Wang, Q. Hao, X. Yang, L. Lu and X. Wang, *Electrochem. Commun.*, 2009, **11**, 1158.
20. Y.G. Wang, H.Q. Li and Y.Y. Xia, *Adv. Mater.*, 2006, **18**, 2619.
21. Y. Han, B. Ding and X. Zhang, *J. New Mat. Electr. Syst.*, 2010, **13**, 315.
22. J. Yan, T. Wei, B. Shao, Z. Fan, W. Qian, M. Zhang and F. Wei, *Carbon*, 2010, **48**, 487.
23. X. Li, X. Wang, L. Zhang, S. Lee and H. Dai, *Science*, 2008, **319**, 1229.

24. M. Cochet, G. Louarn, S. Quillard, J.P. Buisson and S. Lefrant, *J. Raman Spectrosc.*, 2000, **31**, 1041.
25. S. Park and R. S. Ruoff, *Nat. Nanotechnol.*, 2009, **4**, 217.
26. S. Pan and I. A. Aksay, *ACS Nano*, 2011, **5**, 4073.
27. S. N. Kumar, F. Gaillard, G. Bouyssoux and A. Sartre, *Synth. Met.*, 1990, **36**, 111.
28. X. Feng, R. Li, Z. Yan, X. Liu, R. Chen, Y. Ma, X. Li, Q. Fan and W. Huang, *IEEE Trans. Nanotechnol.*, 2012, **11**, 1080.
29. C. W. Kwon, A. Poquet, S. Mornet, G. Campet, J. Portier and J. H. Choy, *Electrochem. Commun.*, 2002, **4**, 197.

Figure Captions:

Figure1. Schematic representation for the fabrication process of PANI-GO/PPy-GO composites.

Figure 2. Cyclic voltammetry (CV) curves of (a) GO, (b) PAG, and (c) PPG.

Figure 3. Raman spectroscopy of GO, PAG, and PPG composites.

Figure 4. X-ray photoelectron spectroscopy (XPS) of composites (a) GO, (b) PAG, and (c) PPG.

Figure 5. Representative SEM images of **(a)** GO, **(b)** PAG, and **(c)** PPG.

Figure 6. Representative TEM images of (a) GO, (b) PAG, and (c) PPG.

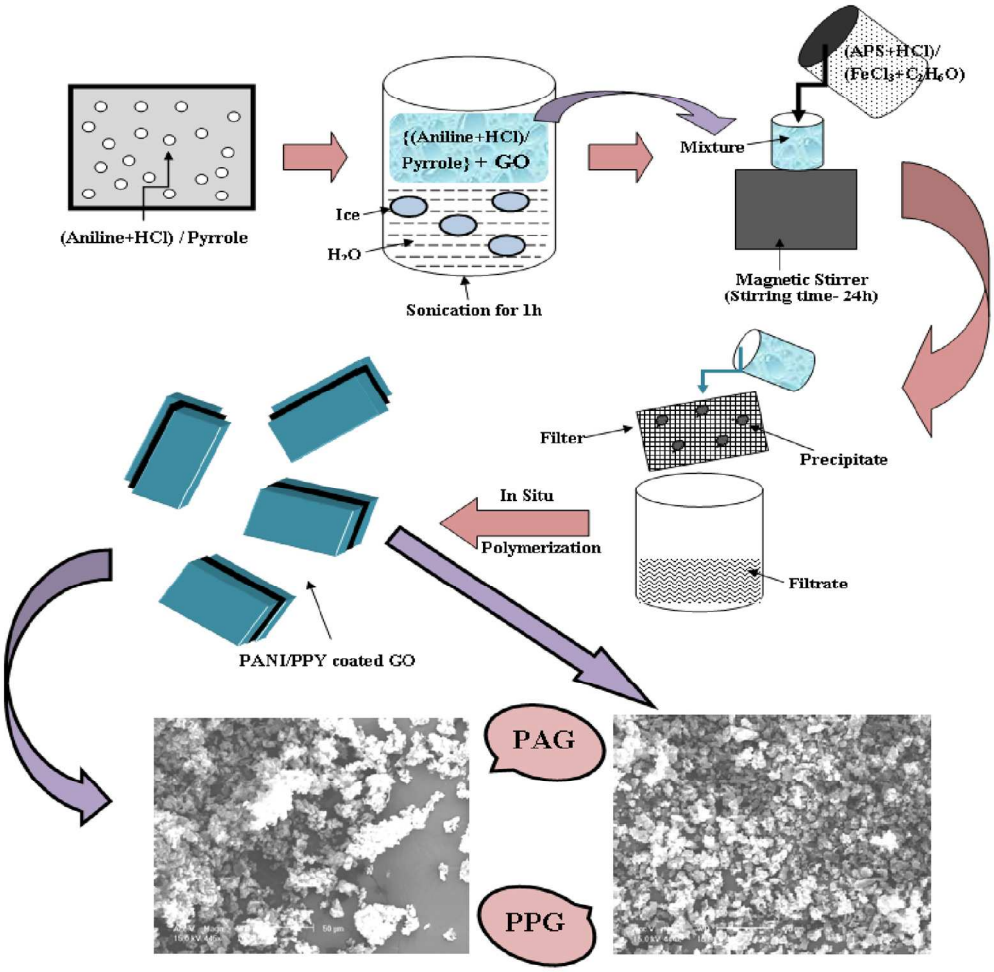

Schematic representation for the fabrication process of PANI-GO/PPy-GO composites.
405x395mm (96 x 96 DPI)

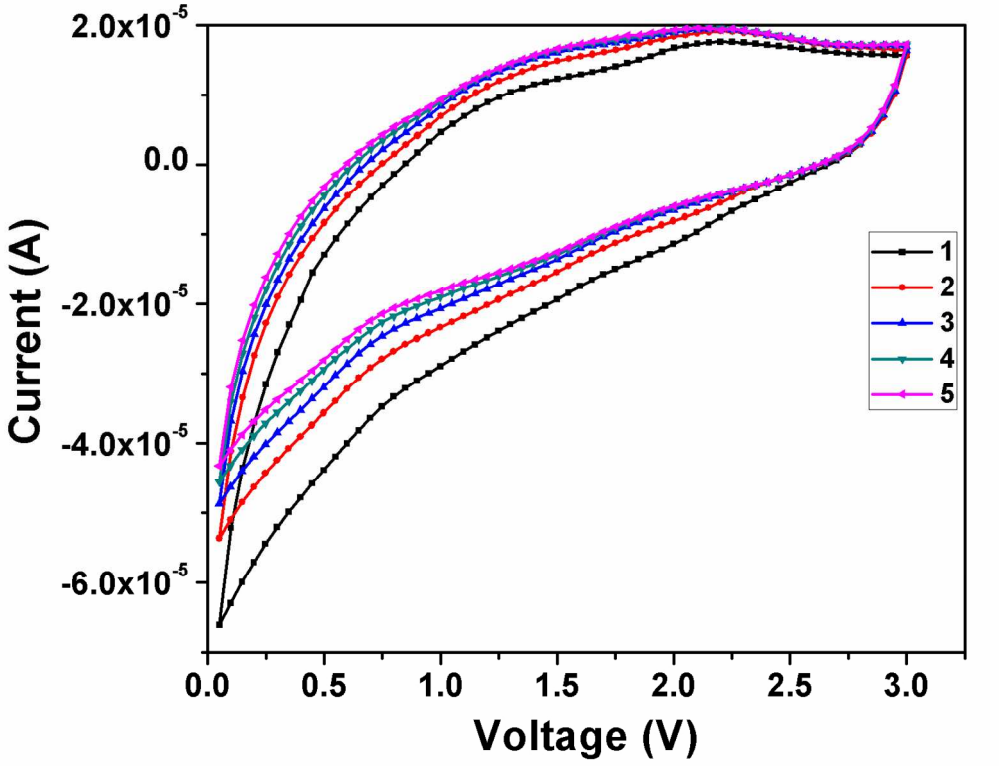

Cyclic voltammetry (CV) curves of GO
289x221mm (150 x 150 DPI)

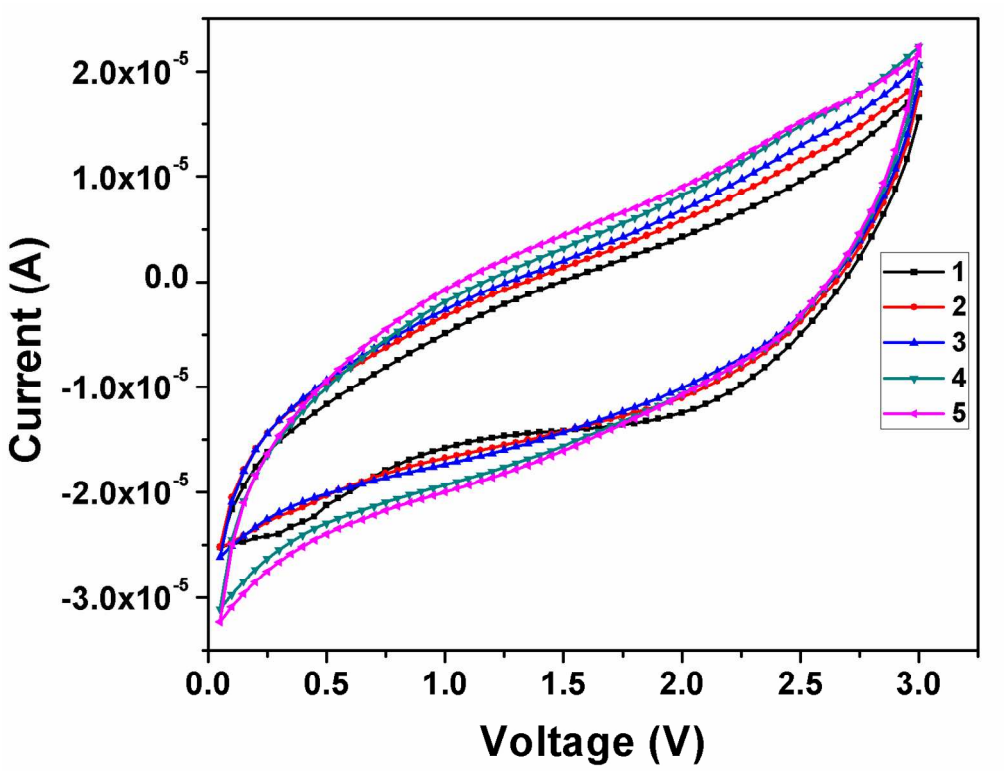

Cyclic voltammetry (CV) curves of PAG
289x221mm (150 x 150 DPI)

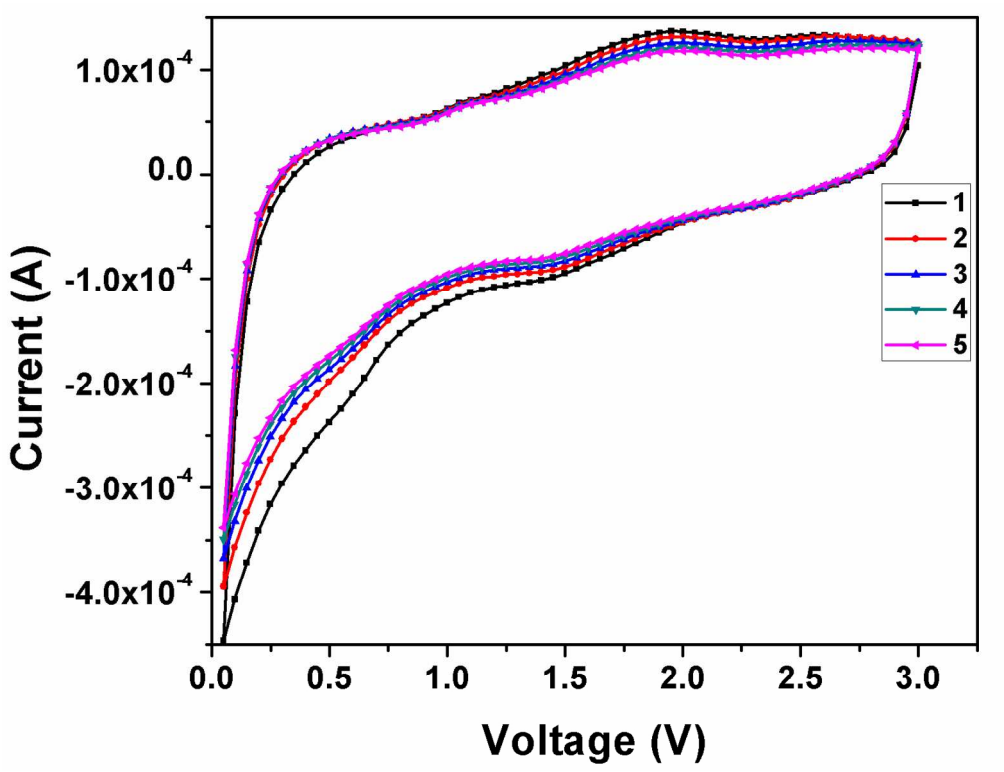

Cyclic voltammetry (CV) curves of PPG
289x221mm (150 x 150 DPI)

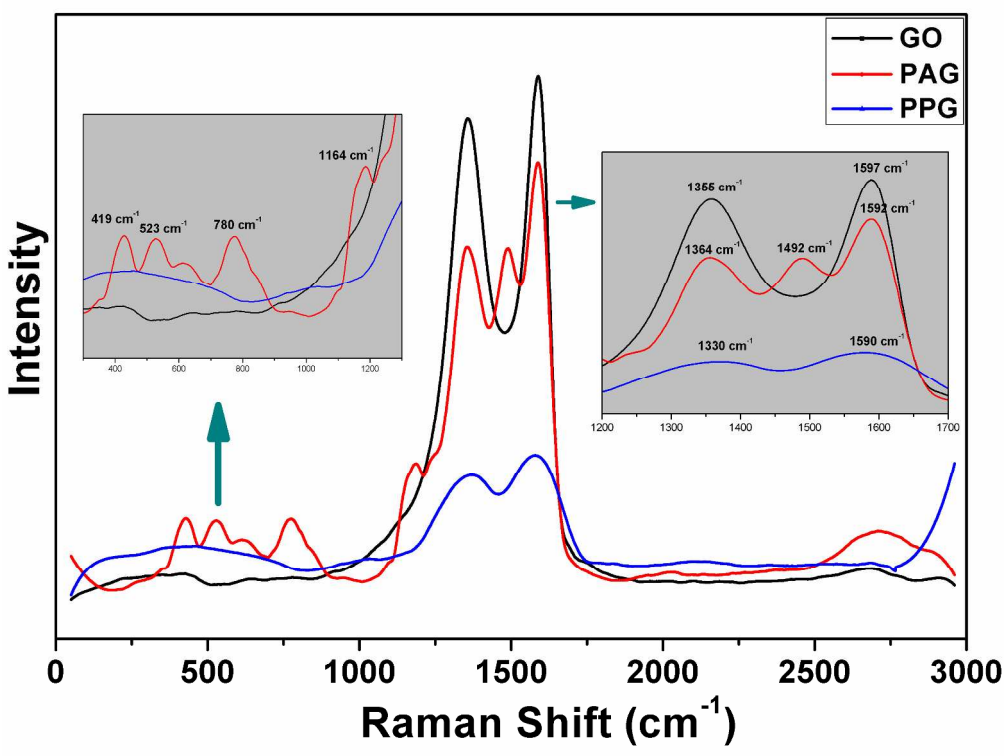

Raman spectroscopy of GO, PAG, and PPG composites
279x212mm (300 x 300 DPI)

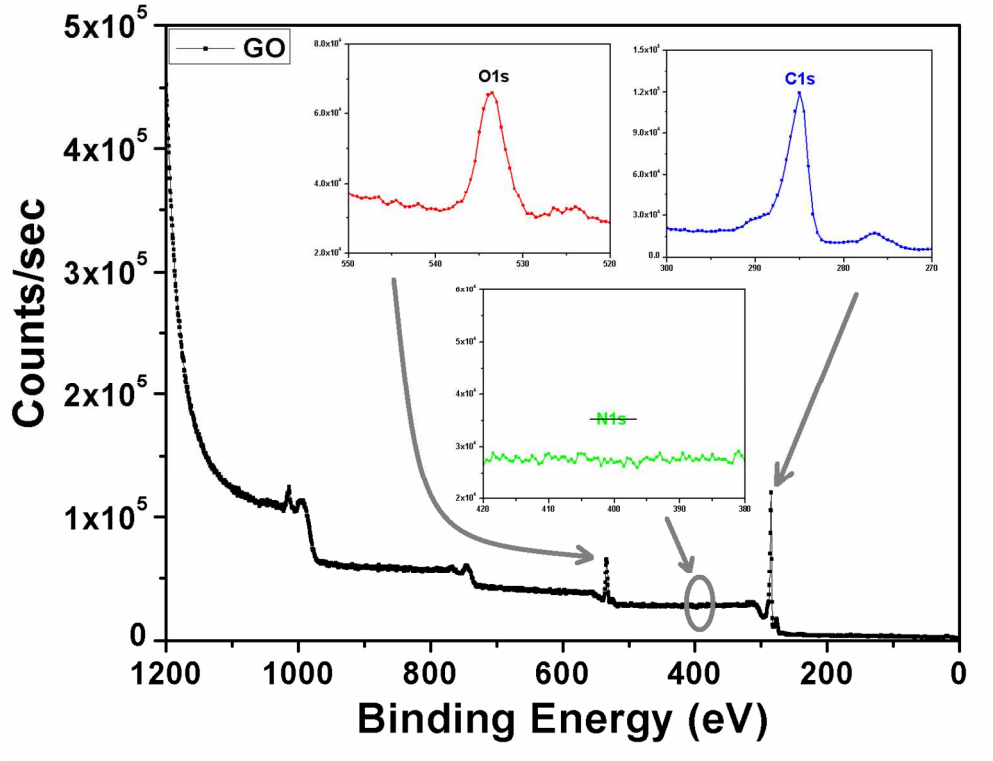

X-ray photoelectron spectroscopy (XPS) of GO
279x212mm (150 x 150 DPI)

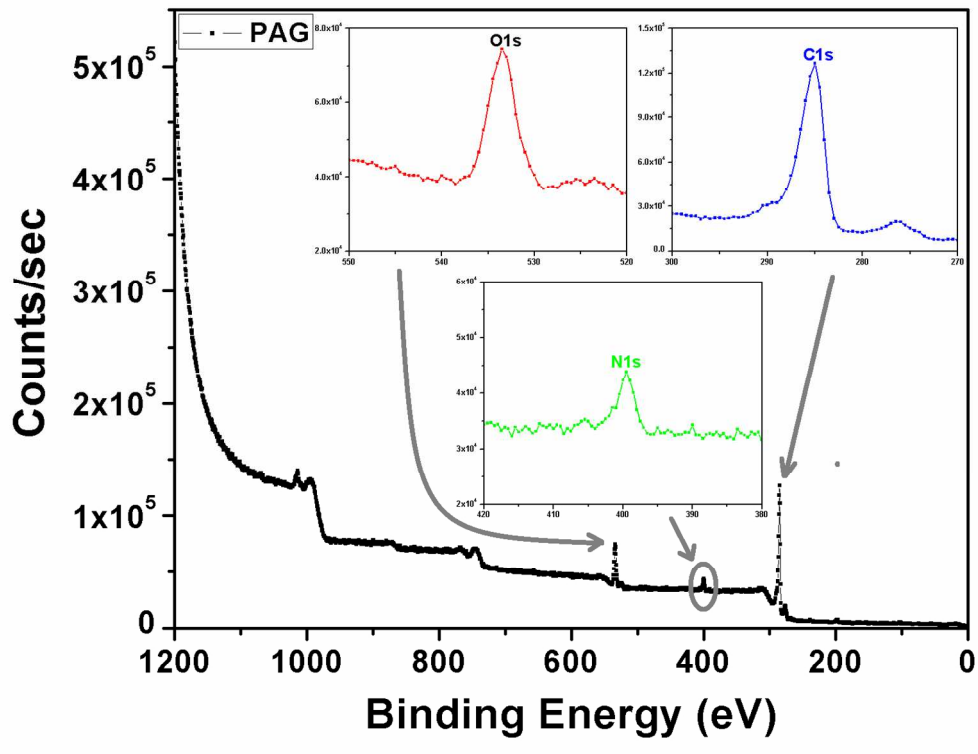

X-ray photoelectron spectroscopy (XPS) of PAG
279x212mm (150 x 150 DPI)

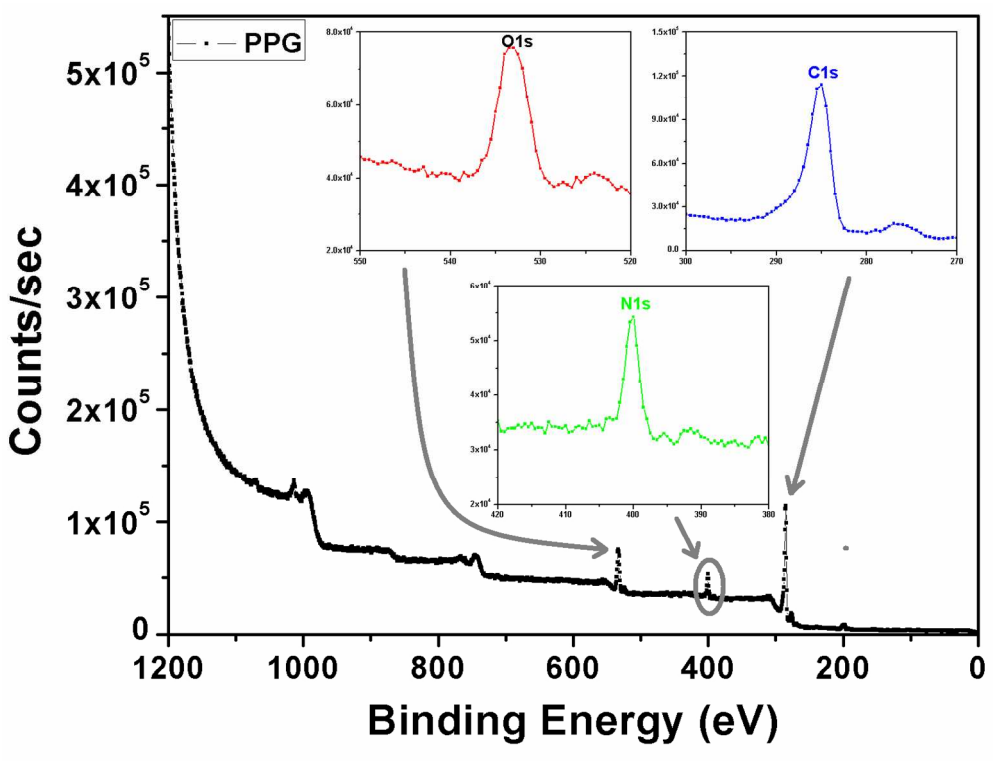

X-ray photoelectron spectroscopy (XPS) of PPG
279x212mm (150 x 150 DPI)

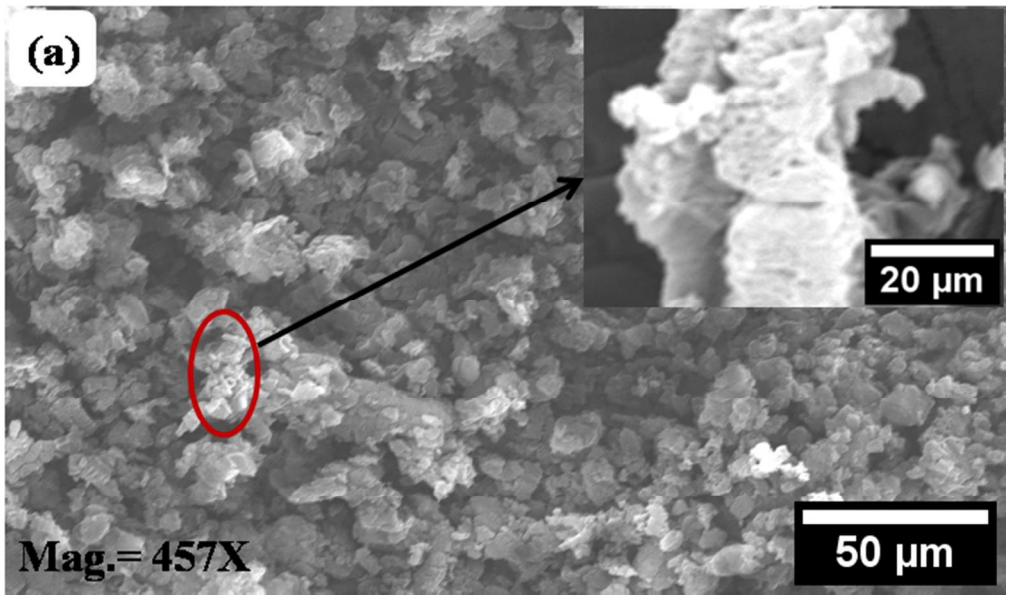

Representative SEM image of GO
188x111mm (96 x 96 DPI)

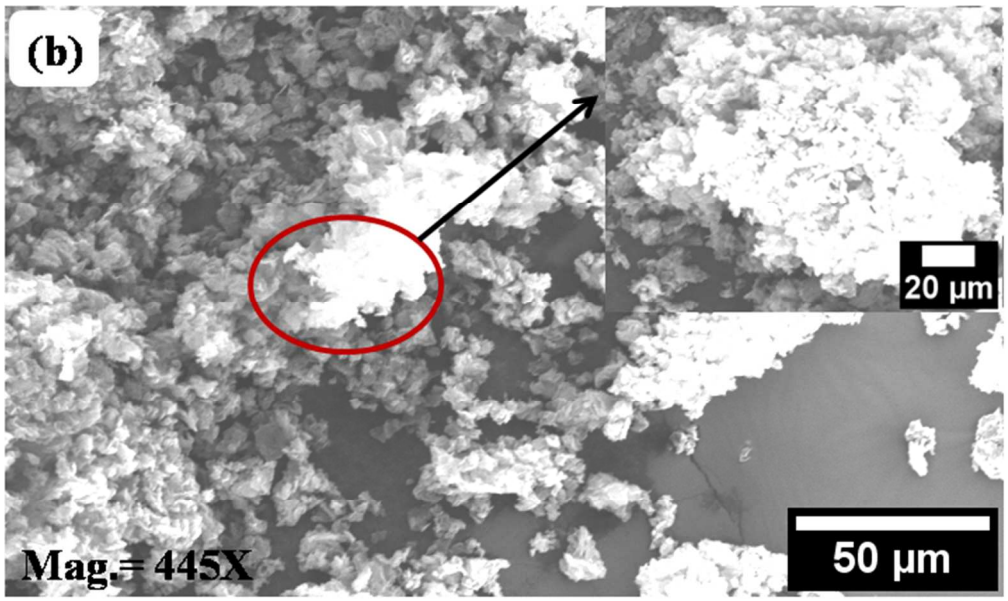

Representative SEM image of PAG
188x112mm (96 x 96 DPI)

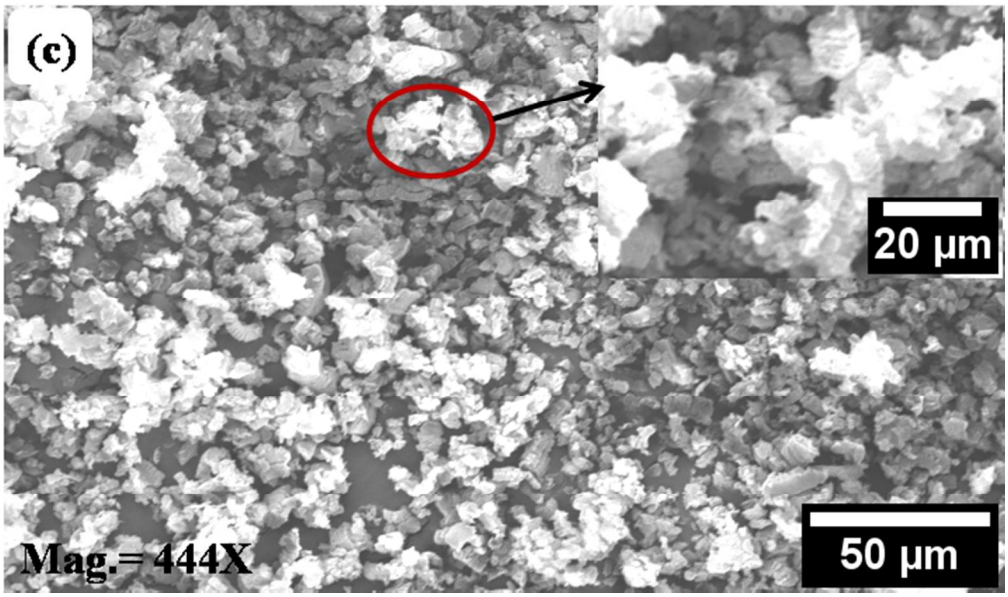

Representative SEM image of PPG
188x111mm (96 x 96 DPI)

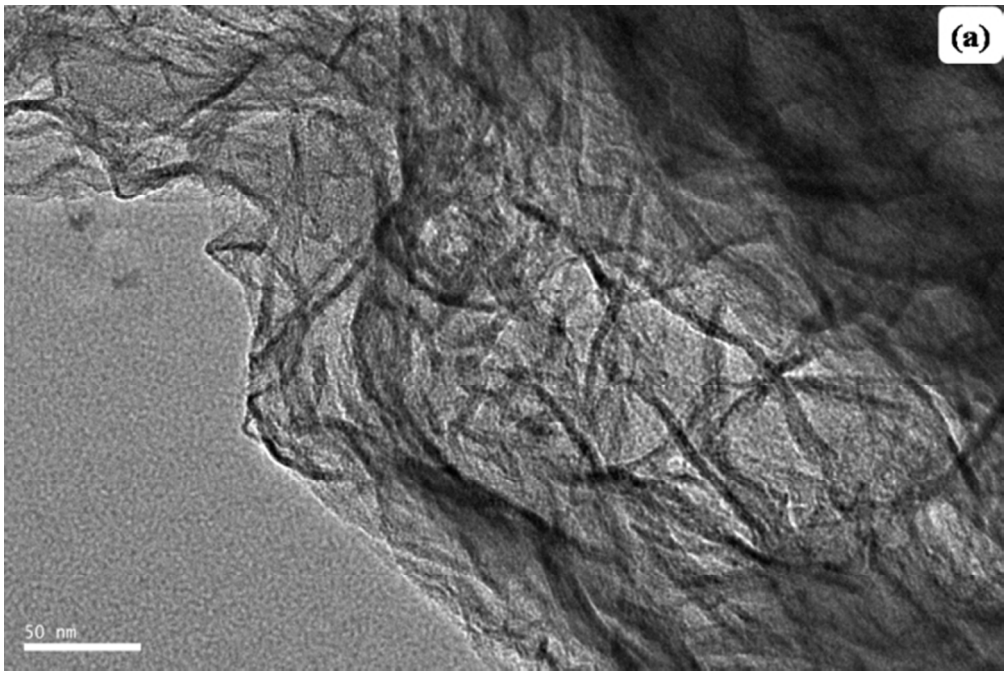

Representative TEM image of GO
190x126mm (96 x 96 DPI)

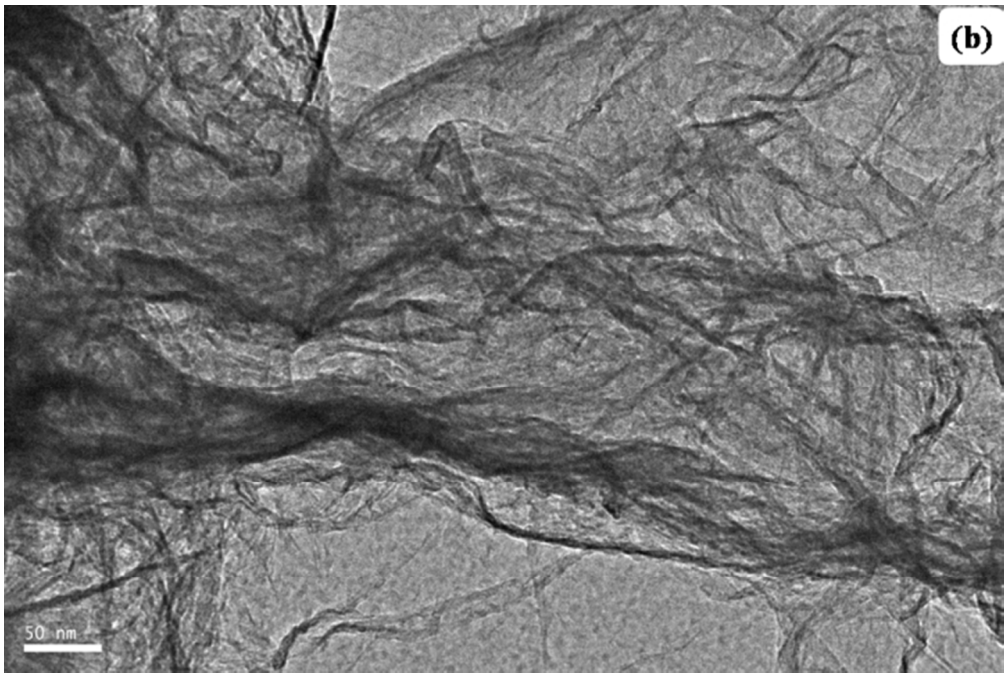

Representative TEM image of PAG
190x127mm (96 x 96 DPI)

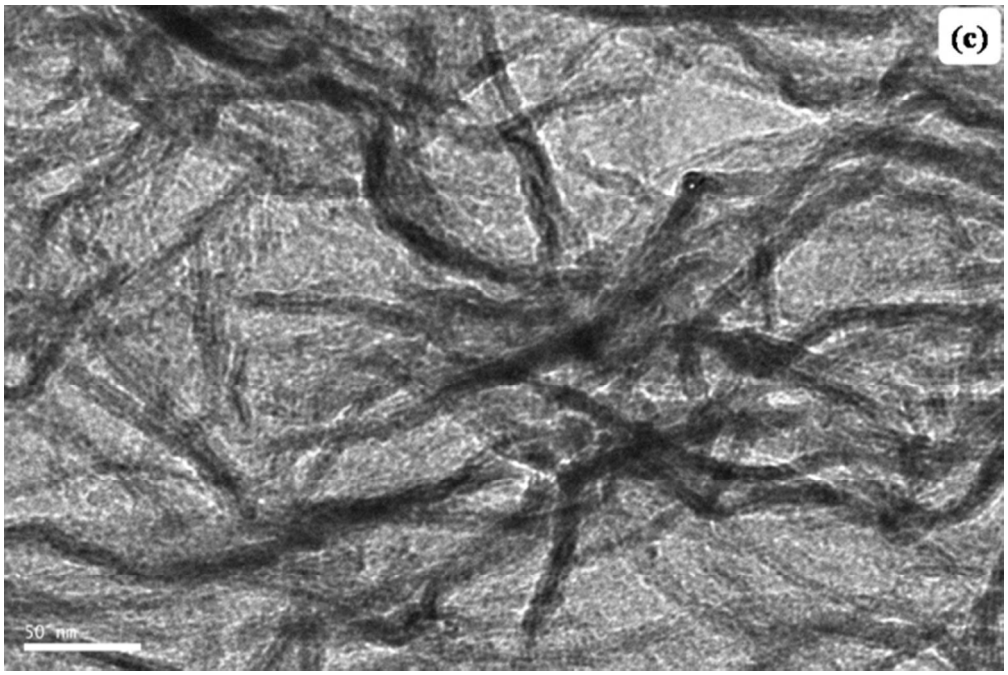

Representative TEM image of PPG
190x126mm (96 x 96 DPI)